


## RESEARCH ARTICLE

# NRF2-mediated SIRT3 induction protects hepatocytes from ER stress-induced liver injury

Ayoung Kim<sup>1,2</sup> | Ja Hyun Koo<sup>2</sup> | Jung Min Lee<sup>2</sup> | Min Sung Joo<sup>2</sup> |  
 Tae Hyun Kim<sup>2,3</sup> | Hyunsung Kim<sup>4</sup> | Dae Won Jun<sup>5</sup>  | Sang Geon Kim<sup>1</sup>

<sup>1</sup>College of Pharmacy and Integrated Research Institute for Drug Development, Dongguk University-Seoul, Goyang-si, South Korea

<sup>2</sup>College of Pharmacy and Research Institute of Pharmaceutical Sciences, Seoul National University, Seoul, South Korea

<sup>3</sup>Research Institute of Pharmaceutical Sciences, College of Pharmacy, Sookmyung Women's University, Seoul, South Korea

<sup>4</sup>Department of Pathology, Hanyang University School of Medicine, Seoul, South Korea

<sup>5</sup>Internal Medicine, Hanyang University School of Medicine, Seoul, South Korea

## Correspondence

Sang Geon Kim, College of Pharmacy,  
 Dongguk University-Seoul, Ilsandong-  
 gu Dongguk-ro 32, Goyang-si,  
 Gyeonggi-do 10326, South Korea.  
 Emails: sgkim@dongguk.edu,  
 sgk@snu.ac.kr

## Funding information

National Research Foundation  
 of Korea (NRF), Grant/Award  
 Number: 2021R1A2B5B03086265,  
 2021R1A6A3A01087745,  
 2021R1C1C1013323 and  
 2021R1A4A5033289

## Abstract

Chronic endoplasmic reticulum (ER) stress in hepatocytes plays a role in the pathogenesis of nonalcoholic fatty liver disease. Therefore, given the association between oxidative stress, mitochondrial dysfunction, and ER stress, our study investigated the role of NRF2-mediated SIRT3 activation in ER stress. SIRT3, a sirtuin, was predicted as the target of NRF2 based on bioinformatic analyses and animal experiments. *Nrf2* abrogation diminished mitochondrial DNA content in hepatocytes with *Ppargc1a* and *Cpt1a* inhibition, whereas its overexpression enhanced oxygen consumption. Further, chromatin immunoprecipitation and luciferase reporter assays indicated that NRF2 induced *SIRT3* through the antioxidant responsive element (ARE) sites comprising the −641 to −631 bp and −419 to −409 bp regions. In tunicamycin-induced ER stress conditions and liver injury animal models following ER stress, NRF2 levels were highly correlated with SIRT3. *Nrf2* deficiency enhanced the tunicamycin-mediated induction of CHOP, which was attenuated by *Sirt3* overexpression. Further, *Sirt3* delivery to hepatocytes in *Nrf2* knockout mice prevented tunicamycin from increasing mortality by

**Abbreviations:** Ad, adenoviruses; ALT, alanine aminotransferase; ANOVA, analysis of variance tests; APAP, acetaminophen; ARE, antioxidant responsive element; BDL, bile duct ligation; BP, biological processes; BW, body weight; CD68, cluster of differentiation 68; ChIP, chromatin immunoprecipitation; ChIP-seq, ChIP-sequencing; CHOP, C/EBP homologous protein; CK19, cytokeratin 19; CPT1a, carnitine palmitoyltransferase 1A; DMEM, Dulbecco's modified Eagle's medium; ER, endoplasmic reticulum; FDR, false discovery rate; FPKM, fragments per kilobase of exon per million reads mapped; GEO, gene expression omnibus; GO, gene ontology; GSEA, gene set enrichment analysis; GTEx, genotype-tissue expression; HSD, honestly significant difference; i.p., intraperitoneally; IACUC, Institutional Animal Care and Use Committee; IRE1α, inositol requiring enzyme 1; KO, knockout; LSD, least significant difference; MCD, methionine/choline-deficient; MF, molecular function; mtDNA, mitochondrial DNA; NAFLD, nonalcoholic fatty liver disease; NASH, nonalcoholic steatohepatitis; NES, normalized enrichment score; NRF2, nuclear factor erythroid 2-related factor 2; OCR, oxygen consumption rate; PBC, primary biliary cholangitis; PERK, protein kinase RNA-like endoplasmic reticulum kinase; PGC1α (*Ppargc1a*), peroxisome proliferator-activated receptor gamma coactivator 1-alpha; qRT-PCR, real-time polymerase chain reaction; ROS, reactive oxygen species; SEM, standard error of the mean; TM, tunicamycin; TUNEL, terminal transferase-mediated dUTP nick-end labeling; UPR, unfolded protein response; Veh, vehicle; WT, wild-type; XBP1s, spliced X-box binding protein.

Ayoung Kim and Ja Hyun Koo contributed equally to this paper.

decreasing ER stress. SIRT3 was upregulated in livers of patients with nonalcoholic liver diseases, whereas lower SIRT3 expression coincided with more severe disease conditions. Taken together, our findings indicated that NRF2-mediated SIRT3 induction protects hepatocytes from ER stress-induced injury, which may contribute to the inhibition of liver disease progression.

#### KEYWORDS

CHOP, ER stress, liver disease, NRF2, SIRT3

## 1 | INTRODUCTION

A significant proportion of individuals in the general population suffer from nonalcoholic fatty liver disease (NAFLD), with a prevalence rate of up to 80%–90% among the obese population.<sup>1</sup> NAFLD ranges from simple steatosis, an early stage of this disease, to nonalcoholic steatohepatitis (NASH), after which it may develop into more severe diseases including fibrosis, cirrhosis, and hepatocellular carcinoma.<sup>2</sup> Hepatocytes are rich in endoplasmic reticulum (ER) and mitochondria due to their high protein synthesis requirements and energy metabolism, and therefore misfolded or unfolded proteins accumulate in the ER when ER homeostasis changes.<sup>3</sup> Consequently, multiple risk factors including ER stress and mitochondrial dysfunction as well as hepatocyte lipotoxicity would contribute to lipid accumulation and the ensuing hepatitis (i.e., NASH).<sup>4</sup>

Oxidative stress and mitochondrial dysfunction are closely linked to each other and may be induced by ER stress in the cell. Particularly, persisting ER stress triggers  $\text{Ca}^{2+}$  overload in mitochondria through ER–mitochondria contact sites and perturbs mitochondrial respiration capacity through the generation of reactive oxygen species (ROS). Therefore, ER stress is associated with mitochondrial dysfunction and may lead to catastrophic cell death if left unattended.<sup>5,6</sup> Based on these premises, it is presumed that mitochondria participate in adaptive responses to ER stress in hepatocytes by determining cell fate after the activation of the unfolded protein response (UPR). Despite the association between mitochondrial ROS and ER stress, the mechanisms by which oxidative stress and its associated adaptive responses contribute to ER stress resolution should be further clarified.

Nuclear factor erythroid 2-related factor 2 (NRF2) has been implicated in the promotion of cell survival in response to ER stress. The phosphorylation of NRF2 by protein kinase RNA-like endoplasmic reticulum kinase (PERK), which belongs to the canonical ER stress pathways, trans-activates a set of antioxidant and detoxifying genes, thus contributing to the maintenance of

sulfhydryl levels in the cell. This mechanism serves as a buffer that prevents the accumulation of ROS during the UPR.<sup>7</sup> However, the molecular and pathological impacts, by which NRF2 exerts an adaptive response to ER stress, remain uncharacterized. Therefore, our study sought to elucidate the effects of NRF2 on mitochondrial biogenesis for the control of oxidative capacity under ER stress conditions.

Several isoforms of sirtuins,  $\text{NAD}^+$ -dependent protein deacetylases, are expressed in the mitochondria and regulate energy metabolism. Here, we found that NRF2 activated SIRT3 (i.e., a mitochondrial sirtuin localized in the mitochondrial matrix) in response to ER stress. SIRT3 deficiency may cause insulin resistance, steatohepatitis, and obesity due to its ability to control mitochondrial capacity<sup>8,9</sup> and oxidative stress.<sup>10,11</sup> Therefore, SIRT3 may play an important role in mitochondrial biogenesis and cytoprotection under pathological conditions characterized by ER stress. Our findings demonstrate the functional role of the NRF2-SIRT3 axis in cell survival under ER stress using bioinformatic datasets, loss- or gain-of-function experiments using in vivo and in vitro models, liver injury animal models with ER stress, and the specimens of NAFLD patients. Our findings thus demonstrate the regulatory role of the NRF2-SIRT3 pathway in mitochondrial capacity control in hepatocytes, the association between NRF2 and SIRT3 expression, and of SIRT3 downregulation with the exacerbation of liver disease accompanying ER stress.

## 2 | MATERIALS AND METHODS

### 2.1 | Materials

Anti-NRF2, anti-SIRT3, anti-spliced X-box binding protein (XBP1s), and anti-inositol requiring enzyme 1 ( $\text{IRE1}\alpha$ ) were obtained from Cell Signaling Technology (Beverly, MA, USA). Anti-GRP78 and anti-cytokeratin 19 (CK19) antibody were supplied by Abcam (Cambridge, MA, USA). Anti-F4/80 and anti-cluster of differentiation 68 (CD68) were obtained from Santa

Cruz Biotechnology (Santa Cruz, CA, USA). Antibody directed against C/EBP homologous protein (CHOP) was obtained from Santa Cruz Biotechnology (CA, USA) or Cell Signaling Technology (MA, USA). Horseradish peroxidase-conjugated goat anti-rabbit and goat anti-mouse IgGs were purchased from Zymed Laboratories (San Francisco, CA). Anti- $\beta$ -actin antibody and other reagents were obtained from Sigma Aldrich (St. Louis, MO, USA).

## 2.2 | Patient samples

The study using human samples was approved by the Institutional Review Boards at Eulji Hospital or Hanyang University Hospital. Liver samples from the patients with NAFLD (or NASH) reported in the previous study were used and the clinical characteristics of the patients and the control groups, and excluding criteria were precisely documented in the report.<sup>12</sup> The protocol was registered at the Clinical Research Information Service (KCT0000900, <http://cris.nih.go.kr/cris/index.jsp>). Histological assessment of liver biopsy samples and the interpretation of immunohistochemical staining (i.e., H-score assignment) were performed as described in the previous work.<sup>12</sup>

## 2.3 | Animals

Animal experiments were conducted under the guidelines of the Institutional Animal Care and Use Committee (IACUC) at Seoul National University. Male mice which have C57BL/6 background except those placed on methionine/choline-deficient (MCD) diet feeding were used for experiments. *Nrf2* knockout (KO) mice supplied by RIKEN BioResource Center (Tsukuba, Japan) were bred and maintained. Mice were maintained in a specific pathogen-free barrier area at ambient temperature ( $22 \pm 2^\circ\text{C}$ ) and humidity ( $55 \pm 10\%$ ), on a 12-h light/dark cycle and fed normal chow diet ad libitum unless otherwise stated. For MCD diet feeding experiments, the 129s1/SvImj mice were started on either a control diet or a MCD diet (Research Diets, New Brunswick, NJ) for 5 weeks. For bile duct ligation (BDL) model, the mice were killed 2 weeks after sham or BDL operation. For the experiment using acetaminophen (APAP), the mice were injected intraperitoneally (i.p.) with a single dose of vehicle or 500 mg/kg APAP. For the induction of ER stress, wild-type (WT) or *Nrf2* KO mice received a single intraperitoneal injection of 2 mg/kg tunicamycin (TM, Sigma Aldrich) in 150 mM dextrose for 48 h, whereas only dextrose solution was injected to control mice. The animals were sacrificed for analysis after appropriate treatments. Blood and tissues

were collected for blood biochemical analyses, protein and RNA quantifications, and histopathological analyses.

## 2.4 | Cell culture and treatment

HEK293 (a human embryonic kidney cell line) and AML12 (a mouse normal hepatocyte-derived cell line) cells were purchased from ATCC (Rockville, MD, USA). The cells were maintained in Dulbecco's modified Eagle's medium (DMEM; Invitrogen, Carlsbad, CA, USA) or 1:1 mixture of DMEM and Ham's F12 medium (Invitrogen) with 0.005 mg/ml insulin, 0.005 mg/ml transferrin, 5 ng/ml selenium, and 40 ng/ml dexamethasone containing 10% fetal bovine serum, 100 units/ml penicillin, and 100  $\mu\text{g}/\text{ml}$  streptomycin at  $37^\circ\text{C}$  in humidified atmosphere with 5%  $\text{CO}_2$ . For all experiments, cells were grown to 70%–80% confluency, and were subjected to no more than 20 cell passages. Mouse primary hepatocytes were isolated from C57BL/6 mice liver by collagenase perfusion and purified by centrifugation under the guidelines of the IACUC, as described previously.<sup>13</sup> Purified primary hepatocytes were placed onto collagen-coated plates ( $5 \times 10^5$  cells/well) in DMEM containing 10% fetal bovine serum, 50 units/ml penicillin, and 50  $\mu\text{g}/\text{ml}$  streptomycin for further analysis. AML12 cells or mouse primary hepatocytes were treated with 2  $\mu\text{g}/\text{ml}$  TM for indicated periods (12 h to 24 h) or with 10 mM sulforaphane for 1 h prior to TM treatment.

## 2.5 | Immunoblot analysis

Protein lysates were resolved by sodium dodecyl sulfate-polyacrylamide gel electrophoresis and immunoblot analyses were performed according to previously published procedures.<sup>13</sup> The bands were visualized using the ECL chemiluminescence Detection Kit (GE Healthcare, UK). Equal loading of proteins was verified by immunoblottings for  $\beta$ -actin. Relative protein levels were determined by scanning densitometry.

## 2.6 | Transient transfection and luciferase reporter assay

Cells were plated at a density of  $1 \times 10^6$  cells/well in 6-well dishes and transfected the following day. The empty plasmid, pcDNA3.1, was used for mock transfection. Briefly, the cells were transfected with 1  $\mu\text{g}$  plasmid encoding for *NRF2* or co-transfected with 1  $\mu\text{g}$  of plasmid encoding for *NRF2* or *SIRT3* promoter-reporter construct with 3  $\mu\text{l}$  of lipofectamine reagent (Life Technologies, Gaithersburg, MD, USA) for 24 h to 48 h. Firefly and Renilla luciferase

activities were measured by using a dual luciferase assay system according to the manufacturer's protocols (GeneCopoeia, Rockville, MD, USA). Otherwise, cells were infected with adenovirus encoding SIRT3 (GFP as control) for 24 h.

## 2.7 | Real-time PCR assays

Total RNA was isolated from cells using an RNeasy mini kit (QIAGEN, Valencia, CA, USA). Isolated RNA (1 µg each) was reverse-transcribed using oligo-d(T)<sub>16</sub> primers to obtain cDNA. Real-time polymerase chain reaction (qRT-PCR) was carried out according to the manufacturer's instructions (Light-Cycler 2.0; Roche, Mannheim, Germany). The relative levels of *Chop*, *Grp78*, *Xbp1s*, or *Sirt1-7* were normalized based on the level of  $\beta$ -actin or 18S ribosomal RNA. After qRT-PCR amplification, a melting curve of each amplicon was determined to verify its accuracy. The primers used for PCR are listed in Table S1.

## 2.8 | Measurement of mitochondrial oxygen consumption rate

Oxygen consumption rate (OCR) was assessed using mitochondrial fractions prepared from HEK293 cells transfected with mock or *NRF2*-expressing vector. After isolation of mitochondrial fractions, protein concentrations in each set of samples were assessed by the Bradford method, as reported previously.<sup>14</sup> Mitochondrial OCR was calculated as an amount of oxygen consumed during a certain period of time normalized with protein contents for each sample using Clark-type electrode in a continuously stirred sealed and thermostatically controlled chamber maintained at 37.8°C (Oxytherm System, Hansatech Instruments Ltd., Norfolk, UK).

## 2.9 | Chromatin immunoprecipitation assays

HEK293 cells were transfected with the plasmid encoding *NRF2* for 48 h, and formaldehyde was added to the cells to a final concentration of 1% for the cross-linking of chromatin. The chromatin immunoprecipitation (ChIP) assay was performed according to the ChIP assay kit protocol (Upstate Biotechnology, Lake Placid, NY, USA). PCR was performed using the specific primers flanking the putative antioxidant response element (ARE) region of the human *SIRT3* gene promoter (ARE-1: sense, 5'-GAAGAACAACCGGGATGTCA-3' and antisense, 5'-CTGCTACGGCGCTCCCAG-3'; ARE-2: sense,

5'-TCACTGGAAACGAGAAGCTTTGGA-3' and antisense, 5'-TCACAGAGGAGGAACTGAAGC-3'; ARE-3: sense, 5'-CCACTCAAGGTTCTCAGCA-3' and antisense, 5'-GAGGAGCGGACCCTTGATG-3'; ARE-4: sense, 5'-CCCGTTAAGGAAGCAGTGAA-3' and antisense, 5'-TGAGGAACCTTGA GTGGCAG-3'; and ARE-5: sense, 5'-TCAACTCCAGACCA TGAGAAAGA-3' and antisense, 5'-GCAAACACACTTT CAGGGCC-3'). An irrelevant region of the gene was PCR amplified as a negative control (sense, 5'-GACAGGAT CTTGCTCTGTTGC-3' and antisense, 5'-GGGATCATTG AGGTCAGGAG-3').

## 2.10 | Hydrodynamic injection of plasmid in mice

For the in vivo experiments, control and *Sirt3*-expressing plasmids were prepared using Endofree-plasmid mega kit (Qiagen, Hilden, Germany). After a week of acclimation, mock or *Sirt3* plasmids (50 µg DNA each) in a total volume equivalent to 10% of the body weight (BW) in PBS were hydrodynamically injected via tail vein of mice within 5–7 s. At 4 days after the injection, mice received a single intraperitoneal injection of TM (2 mg/kg BW, Sigma Aldrich, in 150 mM dextrose) and were sacrificed 3 days thereafter.

## 2.11 | Histological analysis

Liver samples were fixed in 10% formalin, embedded in paraffin, cut into 4-µm thick sections and were mounted on slides. Tissue sections were stained with hematoxylin and eosin for morphology analysis or with Sirius Red for liver fibrosis analysis. For immunohistochemistry, liver sections were stained with antibodies directed against CHOP, SIRT3, GRP78, CK19, F4/80, and CD68.

## 2.12 | TUNEL assays

The terminal transferase-mediated dUTP nick-end labeling (TUNEL) assay was performed as described in the previously work.<sup>13</sup> The assay was done using the DeadEnd Colorimetric TUNEL System, according to the manufacturer's instruction. Liver tissues were fixed in 10% formalin at room temperature for 30 min, and permeabilized with 0.2% Triton X-100 for 5 min. After washing, each sample was incubated with biotinylated nucleotide and terminal deoxynucleotidyl transferase in an equilibration buffer at 37°C for 1 h. The reaction was terminated by incubating the samples in 2× saline sodium citrate buffer for 15 min. Endogenous peroxidases were blocked by treating the samples in 0.3% H<sub>2</sub>O<sub>2</sub> for 5 min, reacted

with horseradish peroxidase-labeled streptavidin solution (1:500), and further incubated for 30 min. Finally, the samples were developed using the chromogen,  $H_2O_2$ , and diaminobenzidine for 10 min.

## 2.13 | Bioinformatic analysis

ChIP-sequencing (ChIP-seq) (GSE37589) data were used to search for NRF2-binding sites to the promoter regions of *sirtuin* family using Integrative Genomics Viewers. Genes positively correlated with *SIRT3* using Pearson correlation (Pearson's coefficients,  $r > 0.5$ ) were analyzed in human liver tissue using Genotype-Tissue Expression (GTEx) v7. Biological process and molecular function (MF) of gene ontology (GO) were analyzed using DAVID v6.8 or g:profiler. Network visualization was performed using Cytoscape v.3.8.2 (STRING or EnrichmentMap plug-in coupled with the AutoAnnotate plug-in). Gene expression data of TM-treated mice (GSE167299, GSE29929), patients with NAFLD (GSE89632, GSE164760, GSE49541), and patients with cirrhosis (GSE25097) were obtained from Gene Expression Omnibus (GEO) available in the public domain. GSE167299 and GSE49541 were analyzed using gene set enrichment analysis (GSEA) v4.1 software, or reactome of canonical pathways and MF of GO (MSigDB, v7.4). False discovery rate (FDR)  $< 0.25$  was used for statistical significance assessment of normalized enrichment score (NES).

## 2.14 | Statistical analysis

Two-tailed Student's *t*-tests or one-way analysis of variance tests (ANOVA) followed by Tukey's honestly significant difference (HSD) or least significant difference (LSD) multiple comparisons correction were done to assess the significance of differences among treatment groups. Data were expressed as the mean  $\pm$  standard error of the mean (SEM). The criterion for statistical significance was set at  $p < .05$  or  $p < .01$ . Coefficient of correlation (*r*) was determined by the Pearson correlation methods.

# 3 | RESULTS

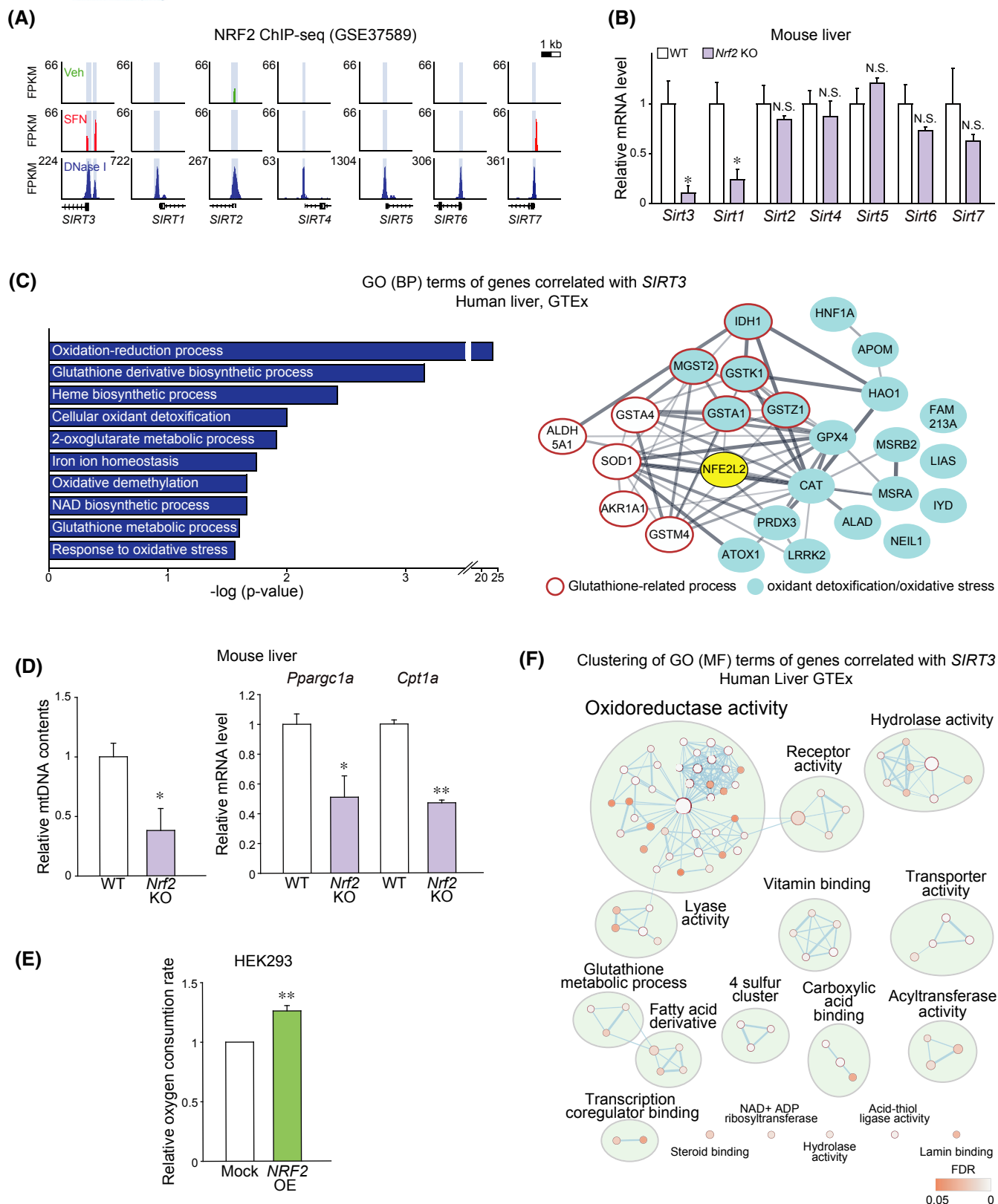
## 3.1 | Association between SIRT3 upregulation and the expression of genes encoding for antioxidative detoxifying enzymes

To elucidate the association between NRF2-dependent antioxidant function and sirtuin expression, we first analyzed a ChIP-seq GEO dataset (GSE37589) from human

lymphoblastoid cells treated with sulforaphane (an electrophilic NRF2 inducer) and found that NRF2 may bind to the promoter regions of *SIRT3* and *SIRT7* (i.e., two mammalian sirtuins) (Figure 1A). In *Nrf2* KO mice, *Sirt3* and *Sirt1* transcript levels were markedly repressed in the liver, whereas others were largely unaffected (Figure 1B). Given that the expression of *SIRT3* was commonly changed in our analyses, in addition to its known role in mitochondrial protection against oxidative stress and metabolic regulation,<sup>15</sup> the functions of this protein were analyzed via GO analysis using the human GTEx dataset. As expected, *SIRT3* in the liver seemed to be closely linked to the genes encoding for oxidation-reduction, glutathione synthetic process, and NRF2-dependent antioxidant systems (Figure 1C). Given the association between NRF2 and *SIRT3*, an isoform localized in mitochondria (Table S2), we next examined the effects of *Nrf2* modulations on mitochondrial biogenesis markers. *Nrf2* deficiency decreased mitochondrial DNA (mtDNA) content in mice livers, with concomitant decreases in *peroxisome proliferator-activated receptor gamma coactivator 1-alpha* (*Ppargc1α*) and *carnitine palmitoyltransferase 1A* (*Cpt1a*) transcript levels (Figure 1D). Consistent with these findings, *NRF2* overexpression enhanced the oxygen consumption rate (Figure 1E). Network analysis of GO terms using the GTEx dataset revealed that several genes linked to *SIRT3* are involved in the "oxidoreductase activity," "glutathione metabolic process," and "hydrolase and transporter activity" pathways (Figure 1F). Together, these results demonstrate the close association between NRF2 and *SIRT3* in the context of mitochondrial biogenesis and antioxidant capacity control in hepatocytes.

## 3.2 | Upregulation of NRF2 and SIRT3 in liver disease animal models with ER stress

Given that oxidative stress participates in the ER stress response, which in turn causes mitochondrial dysfunction, we next examined hepatic NRF2 and *SIRT3* levels in different liver disease animal models accompanying ER stress. Both NRF2 and *SIRT3* were upregulated and were positively correlated with each other in the livers of mice fed with an MCD diet for 5 weeks (Figure 2A). Additionally, representative ER stress markers such as GRP78 and CHOP were all enhanced, thus suggesting the occurrence of ER stress-mediated UPR in the liver. Similar changes were observed in mice subjected to BDL for 2 weeks or a single dose of APAP (500 mg/kg BW, for 6 h) (Figure 2B,C), thus confirming the occurrence of NRF2 and *SIRT3* upregulation during ER stress responses. These results indicate that NRF2 and *SIRT3* levels were highly correlated and increased under ER stress conditions in the liver.



### 3.3 | NRF2/ARE-dependent transcriptional induction of *SIRT3*

To validate the NRF2 regulation of *SIRT3*, we further examined the ability of NRF2 to transcriptionally induce

the *SIRT3* gene. As expected, *NRF2* overexpression increased *SIRT3* mRNA level in HEK293 cells (Figure 3A). Upon analyzing the promoter region of the human *SIRT3* gene up to ~1.5 kb upstream of the transcription start site, five putative ARE sites were identified starting

**FIGURE 1** Association of NRF2 and SIRT3 for mitochondrial activity control. (A) ChIP-seq analyses of NRF2-bound DNA regions around the human *SIRT3* gene promoter regions using a publicly available dataset (GSE37589). DNA fragments immunoprecipitated with basal NRF2 (green peaks) or NRF2 activated with 10  $\mu$ M sulforaphane for 5 h (red peaks). DNase I hypersensitive regions (indicated as blue peaks) were co-aligned to recognize the active promoter regions (blue shades) of each analyzed gene. FPKM, fragments per kilobase of exon per million reads mapped. (B) qRT-PCR assays for *Sirt3* in the liver of wild-type (WT) or *Nrf2* knockout (KO) mice fasted overnight ( $n = 4$  each). (C) Gene ontology (GO) biological processes (BP) associated with *SIRT3*. Genes positively correlated with *SIRT3* (Pearson's coefficients,  $r > 0.5$ ) in human liver tissue based on the data from the Genotype-Tissue Expression (GTEx) database were analyzed using DAVID. Terms related to NRF2 functions are listed ( $p < .05$ ) (left). Network analysis associated with NRF2 (*NFE2L2*) derived from GO (BP) analysis of GTEx (right). The network was analyzed using Cytoscape (STRING plugin). Red circle edge, genes belonging to the "glutathione derivative biosynthetic process" and "glutathione metabolic process" pathways; blue circle, genes belonging to the "cellular oxidant detoxification" and "response to oxidative stress" pathways. (D) qRT-PCR assays for mitochondrial DNA (mtDNA) and *Ppargc1a* and *Cpt1a* transcripts. The relative abundance of mtDNA in mouse livers was normalized by nuclear DNA copy number ( $n = 4$  each, left). qRT-PCR assays for *Ppargc1a* and *Cpt1a* in the liver of mice fasted overnight prior to sacrifice ( $n = 3$  each, right). (E) Relative oxygen consumption rate in HEK293 cells with *Nrf2* (or mock vector) overexpression ( $n = 3$  each). (F) Clustering analysis of GO molecular function (MF) terms for the genes associated with *SIRT3*. MFs of the genes positively correlated with *SIRT3* (Pearson's coefficients,  $r > 0.5$ ) in human liver tissue (GTEx database) subjected to GO analysis using g:profiler. The networks were generated using Cytoscape (EnrichmentMap plug-in coupled with the AutoAnnotate plug-in). Data are reported as the mean  $\pm$  SEM. \* $p < .05$ , \*\* $p < .01$  according to Student's *t*-test (B, D, E)

from  $-39$  bp through  $-1321$  bp (Figure 3B, upper). The ChIP assays indicated that NRF2 was recruited mostly in the regions comprised between  $-641$  bp and  $-631$  bp (site #2) and between  $-419$  bp and  $-409$  bp (site #3) (Figure 3B, lower). NRF2 binding to site #2 was seemingly superior to site #3. Consistent with these findings, analysis of the ChIP-seq database (GSE37589) confirmed that NRF2 tended to preferentially bind to site #2 (Figure 3C). A *SIRT3* promoter-reporter ( $+1$  bp to  $-1200$  bp) and replacement mutant constructs for site #2 and site #3 were then constructed to assess the transcriptional function of the sites (Figure 3D, left). As expected, *NRF2* overexpression significantly promoted luciferase expression in the reporter construct, whereas a mutation at either site #2 or site #3 notably diminished its expression. Moreover, double mutations in both sites completely abolished luciferase induction (Figure 3D, right). These results provide strong evidence that ARE sites spanning from  $-641$  bp to  $-631$  bp and from  $-419$  bp to  $-409$  bp are functionally active for NRF2-mediated *SIRT3* transactivation.

### 3.4 | Induction of NRF2 and SIRT3 by ER stress in liver

Given the role of ER stress in proapoptotic cell fate determination,<sup>5,6</sup> we next examined the effect of TM (an ER stress inducer) treatment on NRF2 and SIRT3. Upon analyzing the GSE167299 dataset derived from livers of mice treated with TM for 12 h, a set of genes involved in the "unfolded protein responses" pathway were found to be enriched (Figure 4A, left). TM treatment for 12 and 6 h caused an increase in *Nrf2* mRNA levels, as demonstrated by the GSE167299 and GSE29929 datasets, respectively (Figure 4A, right and B), thus confirming the ER

stress-driven upregulation of NRF2. To corroborate the induction of SIRT3, we further examined hepatic NRF2 and SIRT3 levels in mice 3 days after a single dose of TM treatment. As expected, the ER stress elicited by TM markedly promoted NRF2 and SIRT3 induction, and the expression of both genes was highly correlated (Figure 4C). TM treatment also increased XBP1s, IRE1, and CHOP levels, which are indicative of ER stress-mediated liver dysfunction. In a cell-based assay using AML12 (a mouse hepatocyte cell line), TM treatment robustly enhanced NRF2 and SIRT3 levels (Figure 4D). Taken together, these data show that ER stress triggers the induction of NRF2 and SIRT3 in hepatocytes.

### 3.5 | Enhanced CHOP induction in *Nrf2* KO mice by ER stress, as antagonized by *Sirt3* overexpression

To assess the protective effects of NRF2 and SIRT3 against ER stress in the liver, we next monitored hepatic ER stress responses using *Nrf2* KO mice. Particularly, we assessed the levels of CHOP (a cell death marker that responds to ER stress), as well as GRP78. *Nrf2* deficiency increased the basal CHOP expression and significantly enhanced the ability of TM to upregulate CHOP and GRP78 in the liver (Figure 5A). We then confirmed that TM increased the expression of ER stress markers more strongly in *Nrf2* KO primary hepatocytes compared to WT hepatocytes (Figure 5B). In contrast, either sulforaphane treatment or *Nrf2* overexpression exerted the opposite effect in AML12 cells (Figure 5C), confirming that NRF2 may have an inhibitory effect on CHOP induction in hepatocytes in response to ER stress. Next, we sought to determine whether *Nrf2* inhibition of CHOP is mediated by SIRT3. As expected, adenoviral

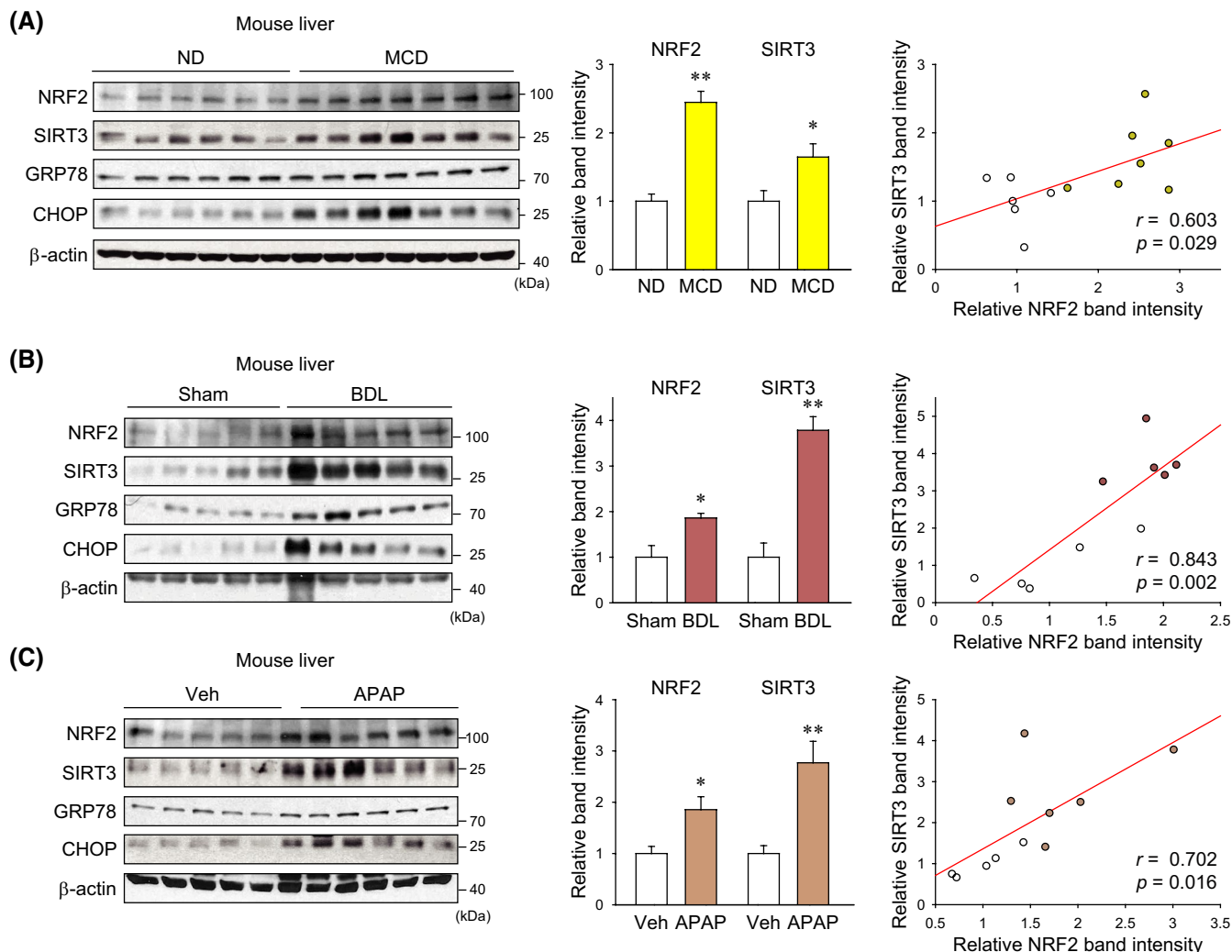


**FIGURE 2** NRF2 and SIRT3 levels in liver injury animal models with ER stress. (A–C) Immunoblots for NRF2, SIRT3, and ER stress markers in liver homogenates (*left*), quantification (*middle*), and correlation plots (*right*) in mice fed with a normal diet (ND) or a methionine/choline-deficient diet (MCD) diet for 5 weeks ( $n = 6, 7$ ) (A); mice submitted to a sham or bile duct ligation (BDL) for 2 weeks ( $n = 5$  each) (B); and mice treated with a single dose of vehicle or acetaminophen (APAP, 500 mg/kg, for 6 h) ( $n = 5, 6$ ) (C). Data are reported as the mean  $\pm$  SEM. \* $p < .05$ , \*\* $p < .01$  according to Student's *t*-test or Pearson's correlation. Veh, vehicle

overexpression of *Sirt3* prevented TM from inducing *Chop*, *Xbp1s*, and *Grp78* in AML12 cells (Figure 5D), demonstrating the protective role of SIRT3 in ER stress-mediated CHOP induction. Together, these results support the notion that NRF2 may inhibit ER stress-mediated CHOP induction through SIRT3.

### 3.6 | Hepatoprotective effect of *Sirt3* overexpression in *Nrf2* KO mice challenged by ER stress

Hydrodynamic tail vein injection delivers genes mainly into hepatocytes.<sup>16</sup> To gain a better understanding of the hepatoprotective effect of SIRT3 in association with

NRF2, we next employed an *in vivo* hydrodynamic transfection technique prior to TM treatment (Figure 6A, *upper*). Hydrodynamic delivery of *Sirt3* through the tail vein successfully increased SIRT3 protein levels in the livers of mice (Figure 6A, *lower*). A single TM dose (2 mg/kg BW) largely decreased the survival rate of *Nrf2* KO mice 3 days after its administration; however, the all of WT mice survived (Figure 6B). More importantly, *Sirt3* overexpression entirely prevented TM-induced mortality in *Nrf2* KO mice. *Sirt3* overexpression decreased serum aspartate transaminase activity in *Nrf2* KO mice treated with TM (data not shown,  $\Delta 56.6\%$ ,  $p < .01$ ) but no significant change was observed for serum alanine aminotransferase (ALT) (data not shown) ( $n = 3$ –11/group). In this experimental set, we thus examined histopathological changes

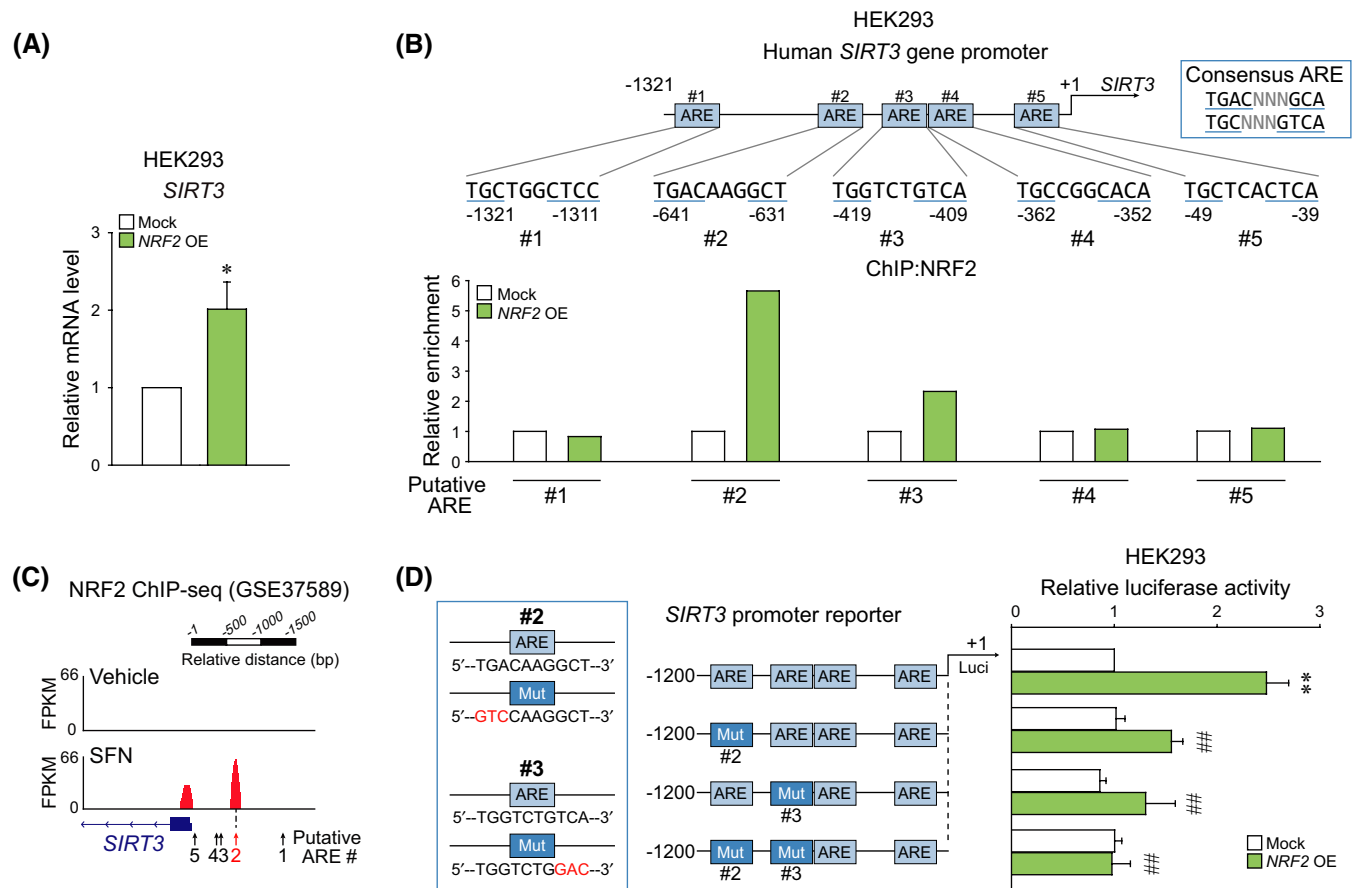


**FIGURE 3** Identification of ARE DNA-binding sites in the promoter region of *SIRT3* gene. (A) qRT-PCR assay for *SIRT3* in HEK293 cells with *NRF2* overexpression for 24 h ( $n = 5$  each). (B) ChIP assays for *NRF2* and putative antioxidant responsive element (ARE) sites in the promoter regions of the human *SIRT3* gene. The lysates of HEK293 cells transfected with *NRF2* for 48 h were subjected to ChIP assays ( $n = 3$  each). (C) Analysis of ChIP-seq dataset (GSE37589) for *NRF2*-binding *SIRT3* DNA regions in human lymphoblastoid cells treated with sulforaphane for 5 h (or vehicle). The arrows indicate putative ARE sites examined in panel B. FPKM, fragments per kilobase of exon per million reads mapped. (D) *SIRT3* luciferase reporter assays ( $n = 4$  each). HEK293 cells were transfected with the respective luciferase reporter comprising the *SIRT3* promoter with or without mutations on ARE site #2 and/or site #3. Putative ARE sites and mutants are depicted as “ARE” boxes and “Mut” boxes, respectively. Data are reported as the mean  $\pm$  SEM. \* $p < .05$ , \*\* $p < .01$ ; ## $p < .01$ , significant differences compared to the WT promoter luciferase. Statistical analyses were conducted using Student's *t*-test (A) or one-way ANOVA coupled with Tukey's HSD (D)

to evaluate full pathology; as expected, *Sirt3* overexpression attenuated liver damage and lipid accumulation in TM-treated *Nrf2* KO mice (Figure 6C). Neither fibrosis (Sirius Red staining) nor ductular reaction (CK19 marker as proliferation of reactive biliary epithelial cells) differed significantly among the groups (Figure S1A,B). The ability of TM to increase CHOP intensities or *Chop*, *Xbp1s*, and *Grp78* transcript levels in either WT or *Nrf2* KO animals was antagonized by *Sirt3* overexpression in the liver (Figure 6D,E). Further, *Sirt3* overexpression diminished inflammation markers (F4/80 and CD68) and the TUNEL intensities associated with TM treatment in the liver of WT and *Nrf2* KO mice (Figures S1C,D, and 6F). Additionally, these data provide strong evidence that *Sirt3* overexpression has a protective effect against ER stress-induced liver injury downstream of *NRF2*.

### 3.7 | SIRT3 and ER stress marker levels in patients with liver diseases

*NRF2* activities may increase in hepatocytes of the patients with chronic liver diseases such as primary biliary cholangitis (PBC), viral hepatitis, and alcohol-related liver disease.<sup>17</sup> To validate our findings in liver disease models, we examined *SIRT3* and ER stress marker levels in liver samples of normal subjects and NAFLD patients using immunohistochemical and H-scoring methods. As expected, NAFLD patients exhibited higher H-scores for *SIRT3* and GRP78 than normal subjects (Figure 7A,B). The analysis of GEO datasets (GSE89632 and GSE164760) also elucidated higher *CHOP* and *GRP78* transcript levels in patients with steatosis or NASH compared to healthy individuals (Figure 7C). Consistently,

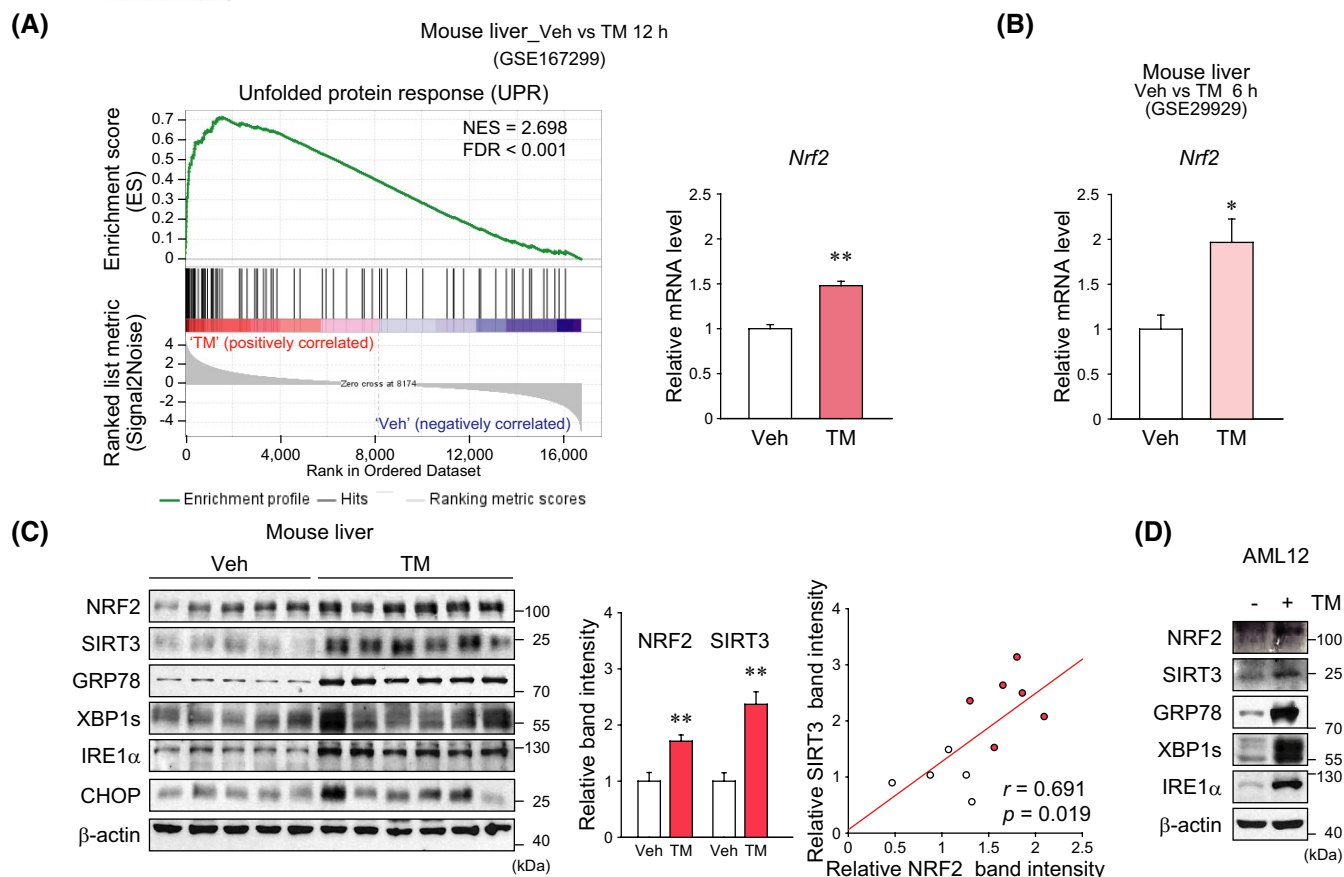


**FIGURE 4** Upregulation of NRF2 and SIRT3 by ER stress inducer. (A) Gene set enrichment analysis (GSEA) showing positively enriched gene signatures in the liver of mice treated with tunicamycin (TM; GSE167299, 2.5 mg/kg, 12 h). The data were analyzed using the reactomes of curated gene sets (left). qRT-PCR assay for *Nrf2* in the liver of mice subjected to vehicle or TM (right) treatment ( $n = 3$  each). (B) *Nrf2* transcript levels using the GSE29929 dataset obtained from the liver of mice treated with vehicle or TM for 6 h ( $n = 3, 4$  each). (C) Immunoblots of NRF2, SIRT3, and ER stress markers in liver homogenates (left), quantification of NRF2 and SIRT3 (middle), and their correlation (right). Mice were subjected to a single dose of TM (2 mg/kg, i.p.) and sacrificed 3 days thereafter ( $n = 5, 6$ ). (D) Immunoblots of AML12 cells treated with 2  $\mu$ g/ml TM for 24 h. Data are reported as the mean  $\pm$  SEM. \* $p < .05$ , \*\* $p < .01$  according to Student's *t*-test (A–C) or Pearson's correlation (C). Veh, vehicle

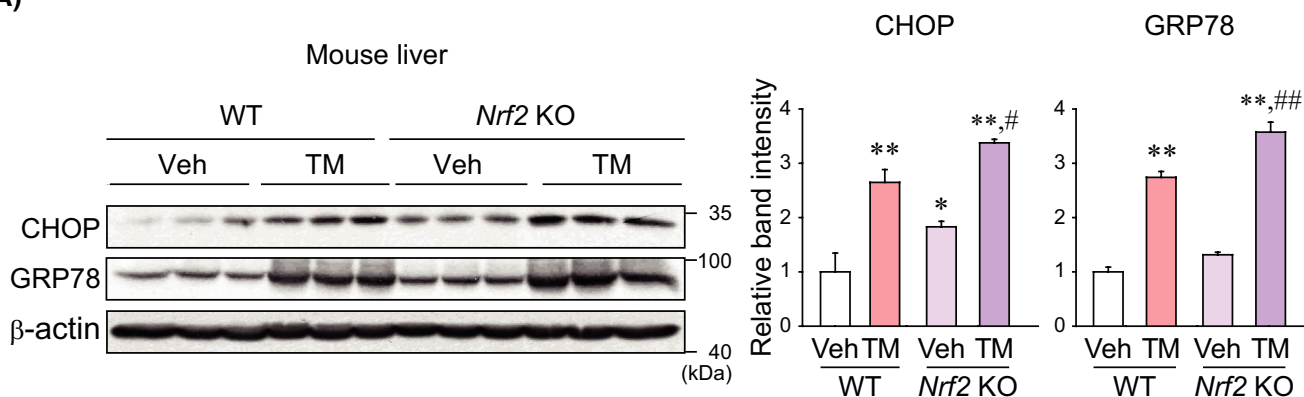
immunohistochemistry of SIRT3 showed a higher intensity in the liver of mice subjected to BDL for 2 weeks than control mice (Figure S2). Further, we examined whether NAFLD severity affected SIRT3 levels by conducting GSEA using the GSE49541 dataset. In the analysis of NAFLD patient population, several genes associated with NAD<sup>+</sup>-dependent protein deacetylase were inversely correlated with disease severity (Figure 7D, left). Among the examined genes, *SIRT3* mRNA levels were lower in patients with severe NAFLD than those with mild symptoms (Figure 7D, right). Likewise, a subgroup of NAFLD patients with high median SIRT3 H-scores exhibited lower serum ALT activities (Figure 7E, left). Therefore, an inverse correlation was observed between the serum ALT activity and *SIRT3* level (Figure 7E, right). Moreover, analysis of the GSE25079 database indicated that patients with cirrhosis also displayed lower hepatic *SIRT3* levels (Figure 7F), confirming the role of SIRT3

repression in liver disease progression. Collectively, our results provide evidence that SIRT3 has a protective effect on the livers of NAFLD patients, and therefore the H-scores of SIRT3 repression may serve as a functional indicator of liver disease progression.

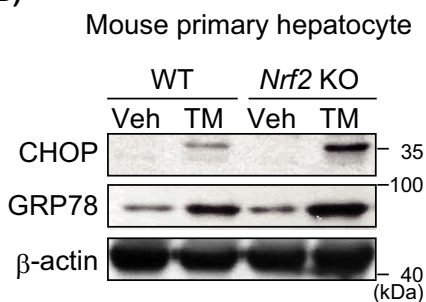
## 4 | DISCUSSION

The ER and mitochondria can modify their structure and function according to environmental cues. ER stress may cause long-term calcium overload and ROS production in mitochondria, thus impairing mitochondrial permeability.<sup>5,6,18</sup> Therefore, ER stress may cause cell death due to mitochondrial dysfunction. Given that mitochondrial dysfunction promotes UPR progression, ER and mitochondria dynamically participate in the maintenance of redox homeostasis.<sup>19</sup> Our study provides evidence that NRF2

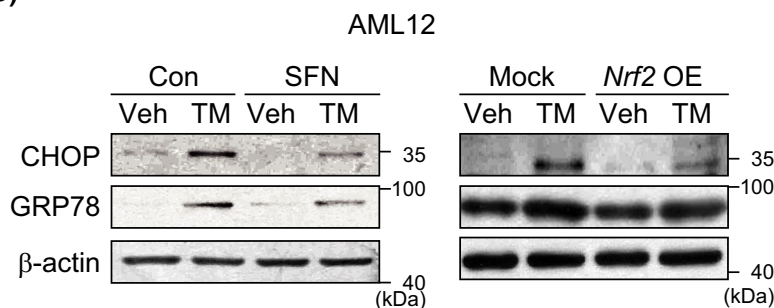
(A)



(B)



(C)



(D)

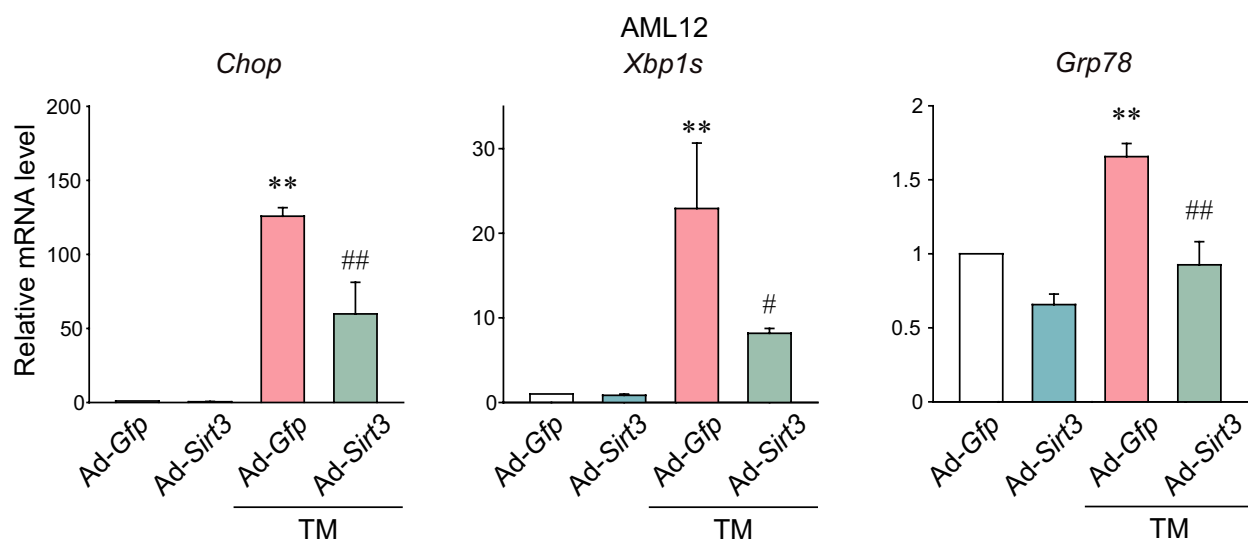


**FIGURE 5** ER stress induction of CHOP in *Nrf2* KO hepatocytes and effects of *Sirt3* overexpression. (A) Immunoblots and their quantifications in livers of mice subjected to a single dose of TM (2 mg/kg BW, i.p.) and sacrificed 3 days thereafter ( $n = 3$  each). (B) Immunoblots for CHOP and GRP78 in mouse primary hepatocytes treated with vehicle or 2  $\mu$ g/ml TM for 18 h. The data were confirmed in a separate experiment. (C) Immunoblots for CHOP and GRP78 in AML12 cells treated with 10 mM sulforaphane (left) or transfected with mock or *Nrf2* plasmid (right) prior to TM treatment (2  $\mu$ g/ml, for 18 h). The data were confirmed in a separate experiment. (D) qRT-PCR assays in AML12 cells infected with adenoviruses (Ad) encoding *Gfp* or *Sirt3* followed by TM treatment (2  $\mu$ g/ml, for 16 h) ( $n = 3$  each). Data are reported as the mean  $\pm$  SEM. \* $p < .05$ , \*\* $p < .01$ ; N.S., not significant; # $p < .05$ , ## $p < .01$ , significant differences compared to TM treatment and/or Ad-*Gfp* infection according to one-way ANOVA coupled with LSD (A,D). Veh, vehicle

induction of SIRT3 plays an important role in overcoming ER stress, thus protecting hepatocytes from ER stress-induced injury.

NRF2 is a transcription factor that maintains proper intracellular redox balance, providing cells with a buffering capacity for redox homeostasis.<sup>20</sup> NRF2 promotes

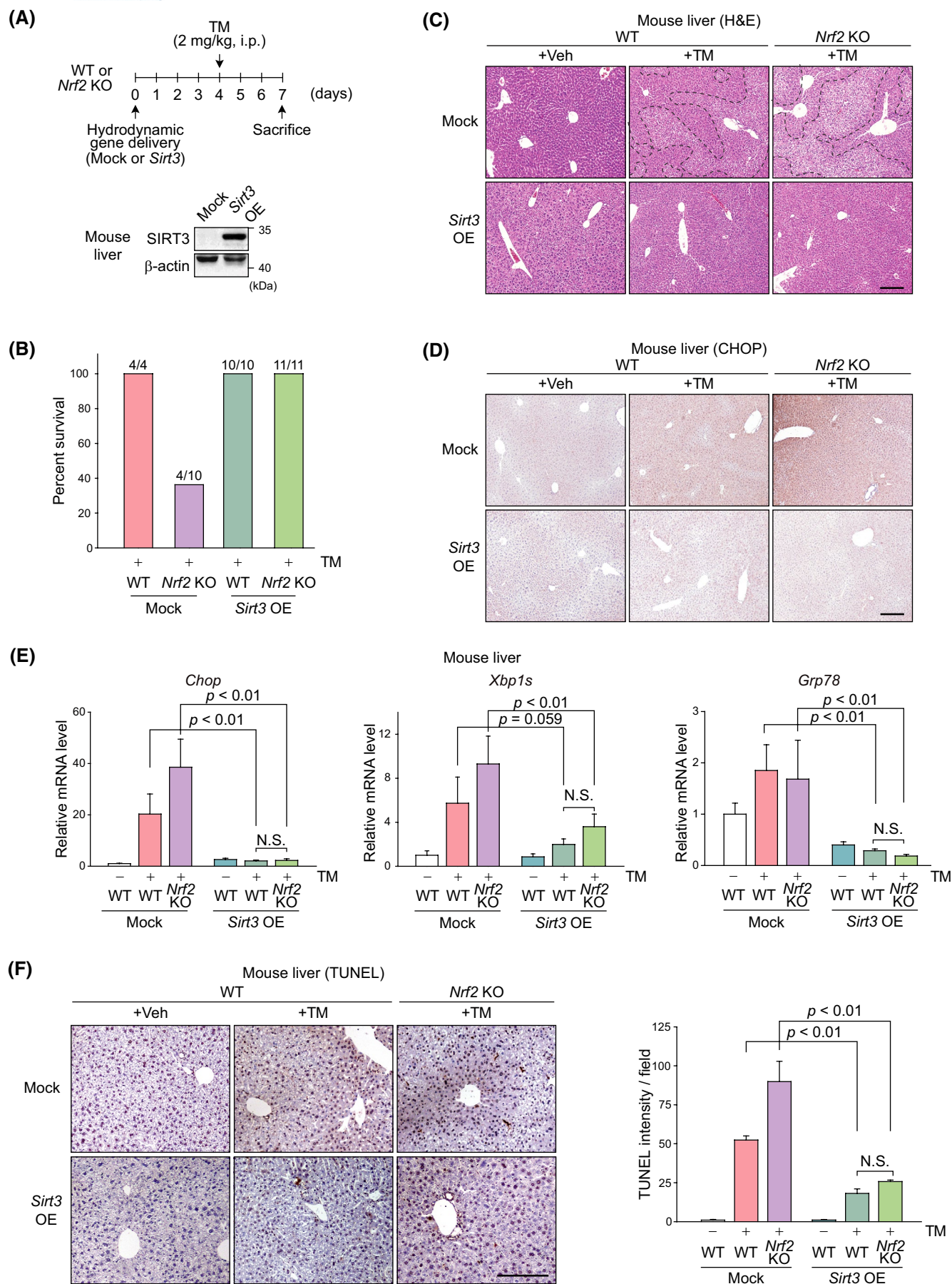


**FIGURE 6** Hepatoprotective effect of *Sirt3* overexpression against ER stress in *Nrf2* KO mice. (A–F) A plasmid encoding for *Sirt3* (or mock vector) was hydrodynamically injected into the mice via the tail vein. After 4 days, the mice were treated with a single dose of TM (2 mg/kg BW, i.p.) and sacrificed 3 days thereafter. (A) Experimental scheme (upper). Immunoblotting assays for SIRT3 (lower). (B) Overall survival rate of the mice ( $n = 4$ –11/group). (C) Representative images of liver histology ( $n = 3$  or 4/group). Damaged areas were marked with dotted lines. Scale bars: 200  $\mu$ m. (D) Representative immunostainings for CHOP ( $n = 3$  or 4/group). Scale bars: 200  $\mu$ m. (E) qRT-PCR assays ( $n = 3$ –11/group). (F) Representative images of TUNEL staining (left) and quantifications (right) ( $n = 3$  or 4/group). Scale bars: 200  $\mu$ m. Data are reported as the mean  $\pm$  SEM. \* $p < .05$ , \*\* $p < .01$ ; N.S., not significant; significant differences between each group were identified via one-way ANOVA coupled with LSD (E,F). H&E, hematoxylin and eosin; Veh, vehicle

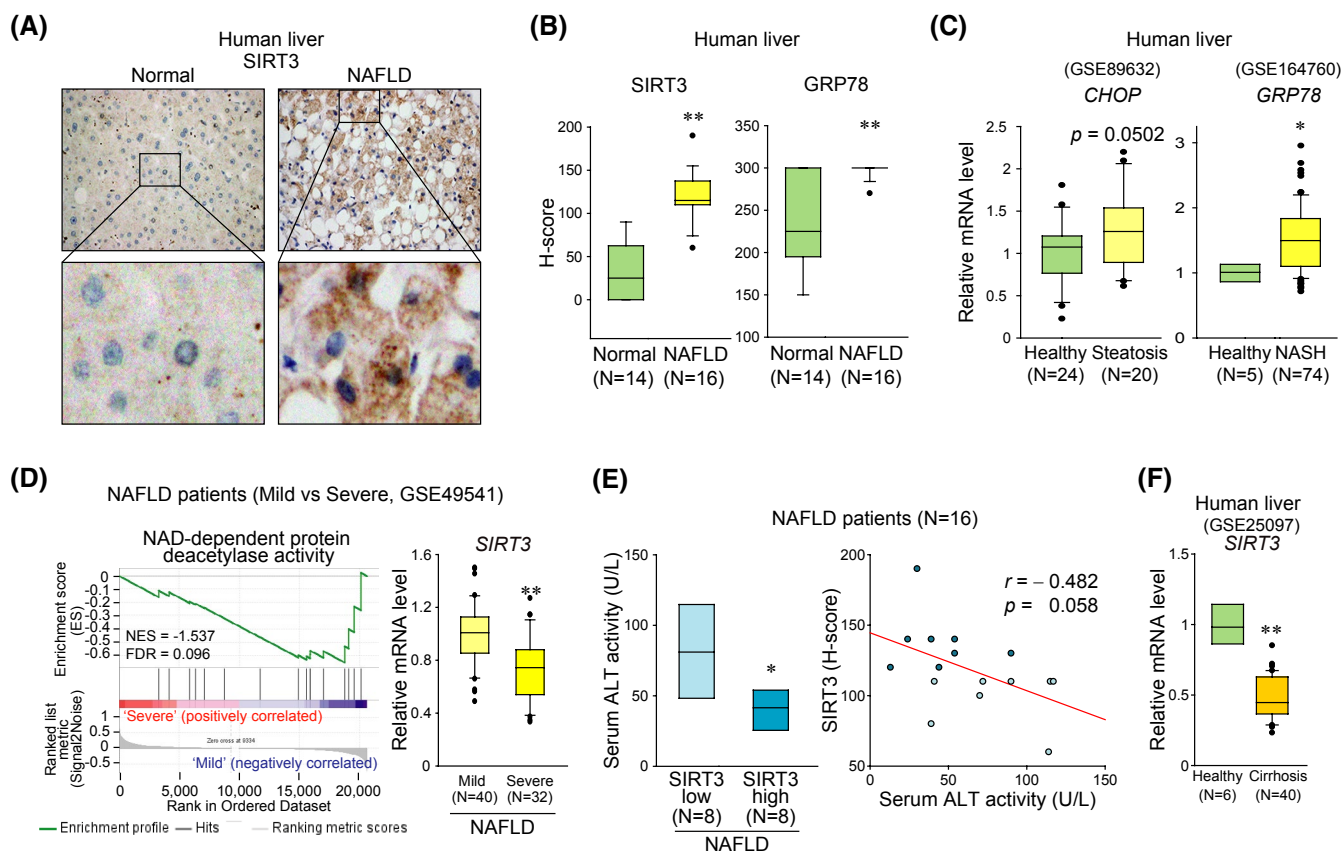


**FIGURE 7** SIRT3 upregulation in NAFLD patients with ER stress, and SIRT3 repression in more severe liver diseases. (A,B) Representative immunostainings for SIRT3 (A) or H-scores of SIRT3 or GRP78 (B) in healthy individuals or patients with NAFLD ( $n = 14$ , 16). SIRT3 and GRP78 levels were semiquantitatively assessed using immunohistochemical staining intensities, percentage of positive cells, and H-scores. Magnification, 400 $\times$ . (C) *CHOP* transcript levels in the livers of healthy individuals or patients with steatosis (GSE89632,  $n = 24$ , 20 each). *GRP78* transcript levels were assessed using GSE164760 from healthy individuals or patients with NASH ( $n = 5$ , 74). (D) GSEA plot showing the inverse correlation of NAFLD severity with the gene signature in GSE49541 ( $n = 40$ , 32). NAD<sup>+</sup>-dependent protein deacetylase activity was assessed using the MF GO set (left). *SIRT3* mRNA levels were assessed using the same dataset from patients with mild or severe NAFLD (right). (E) Serum ALT activities in the same NAFLD patients with low or high SIRT3 as in panel A (Median,  $n = 8$  each). SIRT3 levels were semiquantitatively assessed based on immunohistochemical staining intensities, percentage of positive cells, and the assigned H-scores (left). Correlation between serum ALT activity and SIRT3 H-scores ( $n = 16$ ) (right). (F) *SIRT3* transcript levels were assessed using the GSE25097 dataset from healthy individuals or patients with cirrhosis ( $n = 6$ , 40). The data are shown as a box and whisker plot. Box, interquartile range (IQR); whiskers, 5–95 percentiles; horizontal line within the box, median. \* $p < .05$ , \*\* $p < .01$ , according to Student's *t*-test (B–F) or Pearson's correlation (E)

the expression of target proteins that mediate cellular sulfhydryl production, which is necessary for the protection of cells and organs against ROS. Our analysis of the GTEx dataset elucidated several significantly enriched GO

terms, including “glutathione metabolic process,” “heme biosynthetic process,” “response to oxidative stress,” and “oxidant detoxification,” and identified a positive correlation between SIRT3 and target genes of NRF2 involved in

the oxidoreduction process, thus confirming the close link between NRF2 and SIRT3.

Moreover, our findings indicated that *Nrf2* abrogation diminished mtDNA content in hepatocytes with *Ppargc1α* and *Cpt1a* inhibition, whereas its overexpression enhanced oxygen consumption rate, thus confirming the *bona fide* regulatory effect of NRF2 on mitochondrial energy metabolism. PGC1α and its binding partners (i.e., ERRα and GABP) are known to participate in the induction of SIRT3, whereas SENP1 de-SUMOylates SIRT3 for mitochondrial biogenesis.<sup>21–23</sup> Combined with our GO network analysis results, these findings support the importance of the NRF2-SIRT3 axis in mitochondrial fuel oxidation.

Our results also confirmed the role of NRF2 as a direct transcription activator of SIRT3 for the regulation of mitochondrial adaptation in response to ER stress. When the present study was being conducted, another study demonstrated that NRF2 interacts with the ARE site of the *SIRT3* gene (–301 bp to –251 bp) in Cr(VI)-transformed human bronchial epithelial cells.<sup>24</sup> From the prediction of five different NRF2 DNA-binding site candidates for *SIRT3* gene induction, we identified two ARE sites spanning from –641 bp to –631 bp and from –419 bp to –409 bp located in the promoter region. Importantly, these findings were also supported by NRF2 ChIP-seq and mutation analyses. The identification of NRF2-binding sites as transcriptional activators of SIRT3 in this study suggests that this pathway has a protective role against ER stress-induced proapoptotic signaling.

In MCD, BDL, or APAP intoxication animal models, NRF2 levels were highly correlated with SIRT3 in the liver with increases in ER stress markers including CHOP. Particularly, CHOP is a known proapoptotic transcription factor, which further supports the effect of ER stress on hepatocyte death. This is consistent with the result of enhanced CHOP induction by ER stress under *Nrf2* deficiency conditions, as well as the outcomes of our *in vivo* experiments (i.e., TUNEL-positive cell numbers), thus confirming that *Nrf2* ablation facilitates ER stress-induced liver injury.

SIRT3 is highly expressed in metabolically active organs such as the liver and plays an important role in controlling energy metabolism through mitochondrial biogenesis.<sup>15</sup> Although the effects of SIRT3 on ER stress-induced lipotoxicity have been studied in neurons, chondrocytes, and pancreatic β-cells,<sup>25–27</sup> its functional role in ER stress response in liver disease was unclear. Our findings show that ER stress significantly increased mortality rates in *Nrf2* KO mice. Concretely, more than half of the *Nrf2* KO mice died from severe ER stress, corroborating the protective role of NRF2 against ER stress-induced mortality. Another important finding of this study was

that *Sirt3* overexpression in the liver rescued the *Nrf2* KO mice from ER stress-induced mortality, which verified the key role of SIRT3 downstream from NRF2 in hepatocyte survival. These results provide key information on SIRT3-mediated regulation of redox state in the cell under ER stress conditions.

Hydrodynamic transfection system delivers genes primarily into hepatocytes at the pericentral region.<sup>16</sup> Using this technique, we found that SIRT3 expression was observed mainly in hepatocytes of the animal BDL model. Consistently, the patients with chronic liver diseases also showed increased NRF2 activity in hepatocytes of the liver,<sup>17</sup> suggesting the role of the NRF2-SIRT3 signaling in hepatoprotection under ER stress conditions. Dysregulation of cholangiocytes is also recognized in cholestatic liver diseases.<sup>28</sup> NRF2 activation in human cholangiocytes was proposed to exhibit a protective effect on biliary epithelial cells from PBC.<sup>29</sup> ER stress-induced CHOP activation is involved in the progression of cholangiopathy.<sup>30</sup> Thus, beneficial effects of SIRT3 in cholangiocytes could also be predictable in PBC accompanying ER stress. A further study determining the physiological relevance of NRF2-SIRT3 pathways in cholangiocytes may be of extra value to understand the role of ER stress in biliary epithelial lesions.

Previous studies have shown that TM causes nuclear translocation of NRF2 through PERK in fibroblast cells, which contributed to cell survival after UPR induction.<sup>7,31</sup> In addition to demonstrating the role of NRF2 as a transcriptional factor for SIRT3, our findings also indicated that patients with more severe liver diseases also exhibited SIRT3 downregulation. Previously, it has been also suggested that NRF2 activity correlated with the grade of inflammation<sup>17</sup> and a decrease in SIRT3 activity is associated with reduced mitochondrial function in fatty liver.<sup>32</sup> Collectively, these findings demonstrated that the NRF2-SIRT3 axis functions as a protective feedback mechanism in response to ER stress in hepatocytes.

Adaptive ER stress can restore ER homeostasis, whereas unresolved ER stress can lead to catastrophic cell death, which illustrates the binary nature of this mechanism.<sup>33,34</sup> ER stress and secondary mitochondrial malfunction are considered risk factors for NAFLD progression.<sup>2</sup> Several studies have linked various liver diseases to both increases and decreases in NRF2 expression. However, recent studies have revealed the activation of NRF2 in patients suffering from chronic liver diseases and inflammation, whereas this gene becomes repressed in more severe conditions such as cirrhosis.<sup>17,35</sup> Here, we demonstrated that ER stress may trigger the progression of NAFLD, which is preceded by decreases in SIRT3 levels during disease progression. Our results demonstrate that *Sirt3* overexpression protected hepatocytes from ER stress, thus ameliorating liver injuries.

Further, this mechanism was activated by NRF2 as substantiated by the results of our in vivo and in vitro studies, supporting that the NRF2-SIRT3 axis may orchestrate UPR and proapoptotic signaling.

The identification of molecules and signaling networks would facilitate the development of novel therapies against metabolic liver diseases. Our analyses of patient samples and public datasets indicated that SIRT3 was adaptively upregulated in patients with steatosis or NASH. More importantly, the finding that SIRT3 levels were lower in severe NAFLD cases or liver cirrhosis supports the notion that dysregulation of the NRF2-SIRT3 pathway may accelerate NAFLD progression. The ability of NRF2 to act as a transcription factor for *SIRT3* implies that NRF2 activation by ER stress mediates the fine-tuning of *SIRT3* level. In turn, this promotes mitochondrial biogenesis and survival, suggesting that the NRF2-SIRT3 pathway acts as a switch control. Therefore, enhancing SIRT3 activity may provide a promising means to treat metabolic liver diseases caused by ER stress. Collectively, our findings demonstrated the ability of SIRT3 to protect hepatocytes from ER stress, thus providing direct evidence for the role of the NRF2-SIRT3 axis in cell protection under ER stress conditions, as well as novel insights into the relationship between ER stress-mediated mitochondrial dysfunction and liver disease progression.

## ACKNOWLEDGMENTS

This work was supported by the National Research Foundation of Korea grants funded by the Korea government (MSIP) (2021R1A2B5B03086265 for S.G.K.; 2021R1A6A3A01087745 for A.K.; and 2021R1C1C1013323 and 2021R1A4A5033289 for J.H.K.).

## DISCLOSURES

The authors declare no conflict of interest.

## AUTHOR CONTRIBUTIONS

The authors contributed in the following way. A.K.: study concept and design, acquisition of data, analysis and interpretation of data, statistical analysis, bioinformatics analysis, drafting of the manuscript. J.H.K.: study concept and design, acquisition of data, analysis and interpretation of data, statistical analysis. M.S.J.: analysis and interpretation of data, bioinformatics analysis, drafting of the manuscript. J.M.L., M.S.J., T.H.K., K.J., and D.W.J.: acquisition of data, analysis and interpretation of data. S.G.K.: study concept and design, analysis and interpretation of data, critical revision of the manuscript for important intellectual content, obtained funding, and study supervision. All authors discussed the results and commented on the manuscript.

## ORCID

Dae Won Jun  <https://orcid.org/0000-0002-2875-6139>

## REFERENCES

1. Younossi Z, Tacke F, Arrese M, et al. Global perspectives on nonalcoholic fatty liver disease and nonalcoholic steatohepatitis. *Hepatology*. 2019;69(6):2672-2682.
2. Baiceanu A, Mesdom P, Lagouge M, Foulfelle F. Endoplasmic reticulum proteostasis in hepatic steatosis. *Nat Rev Endocrinol*. 2016;12(12):710-722.
3. Wang M, Kaufman RJ. Protein misfolding in the endoplasmic reticulum as a conduit to human disease. *Nature*. 2016;529(7586):326-335.
4. Schuster S, Cabrera D, Arrese M, Feldstein AE. Triggering and resolution of inflammation in NASH. *Nat Rev Gastroenterol Hepatol*. 2018;15(6):349-364.
5. Egnatchik RA, Leamy AK, Jacobson DA, Shiota M, Young JD. ER calcium release promotes mitochondrial dysfunction and hepatic cell lipotoxicity in response to palmitate overload. *Mol Metab*. 2014;3(5):544-553.
6. Arruda AP, Pers BM, Parlakg  l G, G  ney E, Inouye K, Hotamisligil GS. Chronic enrichment of hepatic endoplasmic reticulum-mitochondria contact leads to mitochondrial dysfunction in obesity. *Nat Med*. 2014;20(12):1427-1435.
7. Cullinan SB, Diehl JA. PERK-dependent activation of Nrf2 contributes to redox homeostasis and cell survival following endoplasmic reticulum stress. *J Biol Chem*. 2004;279(19):20108-20117.
8. Hirschey MD, Shimazu T, Goetzman E, et al. SIRT3 regulates mitochondrial fatty-acid oxidation by reversible enzyme deacetylation. *Nature*. 2010;464(7285):121-125.
9. Yang W, Nagasawa K, M  nch C, et al. Mitochondrial sirtuin network reveals dynamic SIRT3-dependent deacetylation in response to membrane depolarization. *Cell*. 2016;167(4):985-1000.e21.
10. Liu J, Li D, Zhang T, Tong Q, Ye RD, Lin L. SIRT3 protects hepatocytes from oxidative injury by enhancing ROS scavenging and mitochondrial integrity. *Cell Death Dis*. 2017;8(10):e3158.
11. Someya S, Yu W, Hallows WC, et al. Sirt3 mediates reduction of oxidative damage and prevention of age-related hearing loss under caloric restriction. *Cell*. 2010;143(5):802-812.
12. Ahn SB, Jang K, Jun DW, Lee BH, Shin KJ. Expression of liver X receptor correlates with intrahepatic inflammation and fibrosis in patients with nonalcoholic fatty liver disease. *Dig Dis Sci*. 2014;59(12):2975-2982.
13. Han CY, Rho HS, Kim A, et al. FXR inhibits endoplasmic reticulum stress-induced NLRP3 inflammasome in hepatocytes and ameliorates liver injury. *Cell Rep*. 2018;24(11):2985-2999.
14. Kim TH, Yang YM, Han CY, et al. G  12 ablation exacerbates liver steatosis and obesity by suppressing USP22/SIRT1-regulated mitochondrial respiration. *J Clin Invest*. 2018;128(12):5587-5602.
15. Zhang J, Xiang H, Liu J, Chen Y, He RR, Liu B. Mitochondrial Sirtuin 3: new emerging biological function and therapeutic target. *Theranostics*. 2020;10(18):8315-8342.
16. Chen X, Calvisi DF. Hydrodynamic transfection for generation of novel mouse models for liver cancer research. *Am J Pathol*. 2014;184(4):912-923.

17. Mohs A, Otto T, Schneider KM, et al. Hepatocyte-specific NRF2 activation controls fibrogenesis and carcinogenesis in steatohepatitis. *J Hepatol*. 2021;74(3):638-648.
18. Booth DM, Enyedi B, Geiszt M, Várnai P, Hajnóczky G. Redox nanodomains are induced by and control calcium signaling at the ER-mitochondrial interface. *Mol Cell*. 2016;63(2):240-248.
19. Tabas I, Ron D. Integrating the mechanisms of apoptosis induced by endoplasmic reticulum stress. *Nat Cell Biol*. 2011;13(3):184-190.
20. Niture SK, Jaiswal AK. Nrf2 protein up-regulates antiapoptotic protein Bcl-2 and prevents cellular apoptosis. *J Biol Chem*. 2012;287(13):9873-9886.
21. Kong X, Wang R, Xue Y, et al. Sirtuin 3, a new target of PGC-1 $\alpha$ , plays an important role in the suppression of ROS and mitochondrial biogenesis. *PLoS One*. 2010;5(7):e11707.
22. Satterstrom FK, Swindell WR, Laurent G, Vyas S, Bulyk ML, Haigis MC. Nuclear respiratory factor 2 induces SIRT3 expression. *Aging Cell*. 2015;14(5):818-825.
23. Wang T, Cao Y, Zheng Q, et al. SENP1-Sirt3 signaling controls mitochondrial protein acetylation and metabolism. *Mol Cell*. 2019;75(4):823-834.e5.
24. Clementino M, Kim D, Zhang Z. Constitutive activation of NAD-dependent Sirtuin 3 plays an important role in tumorigenesis of chromium(vi)-transformed cells. *Toxicol Sci*. 2019;169(1):224-234.
25. Yan W-J, Liu R-B, Wang L-K, et al. Sirt3-mediated autophagy contributes to resveratrol-induced protection against ER stress in HT22 cells. *Front Neurosci*. 2018;12:116.
26. Zhang Z, Li M, Ma X, Zhou SL, Ren ZW, Qiu YS. GADD45 $\beta$ -I attenuates oxidative stress and apoptosis via Sirt3-mediated inhibition of ER stress in osteoarthritis chondrocytes. *Chem Biol Interact*. 2018;296:76-82.
27. Zhang H-H, Ma X-J, Wu L-N, et al. Sirtuin-3 (SIRT3) protects pancreatic  $\beta$ -cells from endoplasmic reticulum (ER) stress-induced apoptosis and dysfunction. *Mol Cell Biochem*. 2016;420(1-2):95-106.
28. Banales JM, Huebert RC, Karlsen T, Strazzabosco M, LaRusso NF, Gores GJ. Cholangiocyte pathobiology. *Nat Rev Gastroenterol Hepatol*. 2019;16(5):269-281.
29. Kilanczyk E, Banales JM, Wunsch E, et al. S-adenosyl-L-methionine (SAME) halts the autoimmune response in patients with primary biliary cholangitis (PBC) via antioxidant and S-glutathionylation processes in cholangiocytes. *Biochim Biophys Acta Mol Basis Dis*. 2020;1866(11):165895.
30. Borkham-Kamphorst E, Steffen BT, van de Leur E, Haas U, Weiskirchen R. Portal myofibroblasts are sensitive to CCN-mediated endoplasmic reticulum stress-related apoptosis with potential to attenuate biliary fibrogenesis. *Cell Signal*. 2018;51:72-85.
31. Cullinan SB, Zhang D, Hannink M, Arvisais E, Kaufman RJ, Diehl JA. Nrf2 is a direct PERK substrate and effector of PERK-dependent cell survival. *Mol Cell Biol*. 2003;23(20):7198-7209.
32. Kendrick AA, Choudhury M, Rahman SM, et al. Fatty liver is associated with reduced SIRT3 activity and mitochondrial protein hyperacetylation. *Biochem J*. 2011;433(3):505-514.
33. Hetz C, Papa FR. The unfolded protein response and cell fate control. *Mol Cell*. 2018;69(2):169-181.
34. Han J, Back SH, Hur J, et al. ER-stress-induced transcriptional regulation increases protein synthesis leading to cell death. *Nat Cell Biol*. 2013;15(5):481-490.
35. Wu T, Zhao F, Gao B, et al. Hrd1 suppresses Nrf2-mediated cellular protection during liver cirrhosis. *Genes Dev*. 2014;28(7):708-722.

## SUPPORTING INFORMATION

Additional supporting information may be found in the online version of the article at the publisher's website.

**How to cite this article:** Kim A, Koo JH, Lee JM, et al. NRF2-mediated SIRT3 induction protects hepatocytes from ER stress-induced liver injury. *FASEB J*. 2022;36:e22170. doi:[10.1096/fj.202101470R](https://doi.org/10.1096/fj.202101470R)